NODAL SET OPENINGS ON PERTURBED RECTANGULAR DOMAINS

MARICHI GUPTA

Abstract. In this work, we study the effect of boundary perturbation on the nodal set of Laplacian eigenfunctions on the rectangle. Namely, for a rectangle of a given aspect ratio N, we identify the first Dirichlet mode to feature a crossing in its nodal set, perturb the boundary of the rectangle, and study whether the crossing has opened and if so by how much. The main technique used is an approximate separation of variables that allows us to restrict study to the first two modes in the eigenfunction expansion, and key findings include conditions on the orientation and estimates on the length scale of the opening that depend on the nature of the boundary perturbation. Further, a resonance phenomenon arises where the nodal set changes orientation around appropriate aspect ratios N, independent of boundary perturbation. Applications to Courant Sharp eigenfunctions are discussed, and numeric results supporting our findings are presented.

1. Introduction

Vibration is a fundamental physical phenomenon and mathematicians have spent several decades developing theory and tools to better understand it. Of particular interest in vibrating media are the points that stay fixed during oscillation, called *nodal sets*. These nodal sets depend closely on the geometry of the vibrating object, and a natural question is how exactly the object's shape influences the nodal sets. Closely related to these are *nodal domains*, which are the connected sets of points that do vibrate and are separated by the nodal sets.

There are relations between the mode of vibration and the number of nodal domains. For instance, considering standing waves on a guitar string, or more formally solutions to the Sturm-Liouville problem on the interval, one sees that the k^{th} mode will have k nodal domains, and a nodal set consisting of $k-1$ fixed interior points. We take interest in the fact that the index of the mode, k, is equal to the number of nodal domains.

In higher dimensions, this relation becomes much more interesting and difficult. An early advancement along these lines was Courant's Nodal Domain Theorem, which states that, in any dimension, the k^{th} eigenfunction of the Dirichlet Laplacian will have at most k nodal domains [3]. Very often, it will have less than k nodal domains; whenever it has exactly k nodal domains, we call the corresponding eigenfunction *Courant Sharp*. An early result due to Pleijel states that for any domain in two-or-more dimensions there are only finitely many Courant Sharp modes [9], in contrast with the one-dimensional string, which has infinitely many. For simple domains, there is a complete catalogue of all Courant Sharp modes (e.g. for the Dirichlet unit square, see [9], [2]). Beyond this, however, little is known about what makes a mode Courant Sharp, and the study of Courant Sharp eigenfunctions is an open area of research.

Along a different direction of study, Grieser and Jerison developed in a series of papers a detailed description of the nodal sets of the first and second Dirichlet eigenfunctions on convex domains and domains close to rectangles of high aspect ratios ([5], [6], [7]), along with techniques for performing very detailed analysis of the eigenfunction on the approximately-rectangular domain. The work of Grieser and Jerison was extended by Beck, Canzani, and Marzuola ([1]), who studied the nodal set of the Laplacian on curvilinear rectangles with Dirichlet boundary conditions using similar techniques. Key results from [1] are bounds on the curvature and deviation of the nodal line for the second Dirichlet eigenfunction.

The question explored here is a sort of average of the two earlier ideas - we seek to analyze how domain perturbation decreases the number of nodal domains compared to the corresponding eigenfunction on the unperturbed domain. In particular, for a given rectangle of aspect ratio N, we consider the first

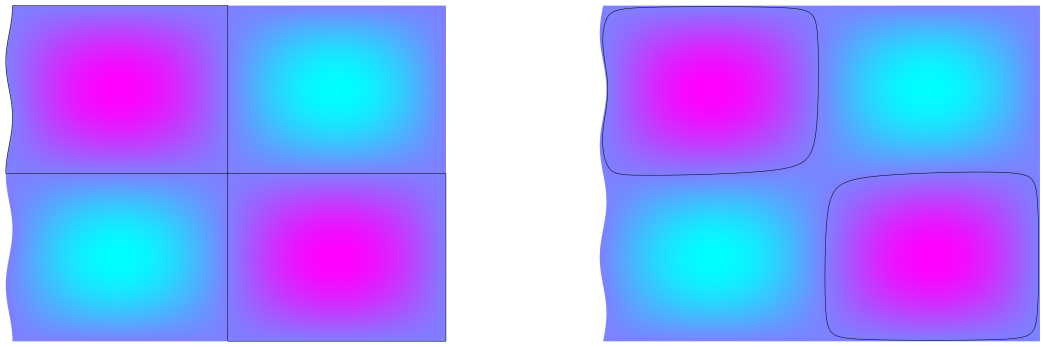

(i) (ii)

FIGURE 1. Eigenfunctions on perturbed rectangles: (i), symmetric perturbation, aspect ratio $N = \sqrt{5/3}$, where the mode of study is Courant Sharp; (ii) asymmetric perturbation, $N = \sqrt{5/3}$.

eigenfunction with a crossing in its nodal set that partitions the rectangle into four nodal domains. We then perturb the boundary of the domain to open the crossing, and study the scale of that opening. We note that mode of study will not always be the fourth eigenfunction itself - that is, our eigenfunction is not necessarily Courant Sharp - but we expect the analysis to transfer over well to crossings that are in Courant Sharp eigenfunctions. We make use of the techniques present in [1] and [7], including the use of the adiabatic ansatz, which is an approximate separation of variables as applied to our domain. The ansatz is a useful one for near-rectangular domains and has, for instance, been used in the study of mathematical billiards [8].

Numerical experiments reveal rich behavior of the eigenfunctions for differing boundary perturbations. For instance, as shown in Figure 1 (i-ii), the magnitude of the opening seems to be impacted by symmetry in the deformation. In (i), no opening is noticeable up to numeric resolution, yet in (ii) an opening connects the two positive components of the eigenfunction. Indeed, we will see that our results allow us to predict these properties for a given boundary perturbation and aspect ratio. While our results are tailored for rectangles of large aspect-ratio, numerical results indicate that our predictions hold well even for moderate aspect-ratios as well (see Section 4 for additional details). With these pictures in mind, we pay close attention to how geometric properties of the domain, such as symmetry in the perturbation and its relative size compared to the rectangle, influence the nodal set opening.

1.1. **Domain and Ansatz Description.** We start by specifying the family of domains, Ω, that are perturbations of the rectangle $[0, N] \times [0, 1]$ for $N > 1$. Let $\phi_L(y)$ be a curve specifying the left side of Ω, and write

$$\Omega = \{(x, y) \in \mathbb{R}^2 \, : \, y \in [0, 1], \phi_L(y) \leq x \leq N\}. \tag{1.1}$$

We require $\phi_L \in C^2([0, 1]; \mathbb{R})$ with $\phi_L(0) = \phi_L(1) = 0$, and to ensure that the domain perturbation is small, we require

$$-\eta \leq \phi_L(y) \leq 0 \text{ for all } y \in [0, 1], \tag{1.2}$$

where $\frac{1}{2} > \eta > 0$ is small. Note that taking $\eta = 0$ forces $\Omega = [0, N] \times [0, 1]$. We highlight two quantities: N, the aspect ratio on the unperturbed rectangle, and the ratio $\frac{\eta}{N}$, which describes the relative size of the side perturbation.

We proceed to identify our eigenfunction of interest, v. To start, consider the Laplacian with Dirichlet boundary conditions on the unperturbed rectangle, $[0, N]\times[0, 1]$ where $N > 1$. That is, consider solutions

to

$$\begin{cases} \Delta\varphi + \lambda\varphi = 0 \text{ in } [0,N]\times[0,1] \\ \varphi = 0 \text{ on } \partial([0,N]\times[0,1]). \end{cases} \tag{1.3}$$

Solutions to this system are described by $\varphi_{n,m}(x,y) = \sin(\frac{n\pi}{N}x)\sin(m\pi y)$, with corresponding eigenvalues $\lambda_{n,m} = \pi^2(\frac{n^2}{N^2} + m^2)$.

We focus on $\varphi_{2,2}(x,y) = \sin(\frac{2\pi}{N}x)\sin(2\pi y)$, with eigenvalue $\lambda_{2,2} = 4\pi^2(\frac{1}{N^2}+1)$. Having chosen Ω, we then take $v(x,y)$ to be the corresponding mode to $\varphi_{2,2}$ that solves

$$\begin{cases} \Delta v + \mu v = 0 \text{ in } \Omega \\ v|_{\partial\Omega} = 0. \end{cases} \tag{1.4}$$

To be precise, the corresponding mode will be the eigenfunction at the same energy level as $\varphi_{2,2}$ - this will hold perfectly so long as η is small enough to not alter the ordering of the modes. We normalize v to ensure $\|v\|_{L^\infty} = 1$, and choose N appropriately to ensure $\lambda_{2,2}$ is a simple eigenvalue.

On the unperturbed rectangle, observe that the nodal set of $\phi_{2,2}$ can be written as $\Gamma_{2,2} = \big([0,N]\times\{\frac{1}{2}\}\big)\cup\big(\{\frac{N}{2}\}\times[0,1]\big)$. In other words, the nodal set of $\varphi_{2,2}$ consists of two lines that intersect in the center of the rectangle and partition it into four connected components. We are thus interested in knowing whether the nodal set of v maintains a crossing in its nodal set, and if not what the size of the opening in the nodal set is. Moreover, we seek information in the orientation of the opening (e.g., whether the connected component in the center runs from the lower-left to upper-right ends of Ω), and the sign of the connected component.

Before we state our main results, it will be helpful to describe our eigenfunction decomposition. We apply the adiabatic ansatz to write

$$v(x,y) = v_1(x)\sin(\pi y) + v_2(x)\sin(2\pi y) + E(x,y), \tag{1.5}$$

where $E(x,y)$ is an error term for small ratio η/N, and where for $k \geq 0$,

$$v_k(x) = 2\int_0^1 v(x,y)\sin(k\pi y)\,dy. \tag{1.6}$$

This ansatz can be viewed as a partial Fourier decomposition with respect to the $y-$axis. The error term $E(x,y) = \sum_{k\geq 3} v_k(x)\sin(k\pi y)$ contains all of the higher modes, and it will be shown in Section 3 that $E(x,y)$ is exponentially small in N. Moreover, $v_1(x)$ and $v_2(x)$ are governed by the ODEs

$$v_1''(x) + \mu_1 v_1(x) = 0 \text{ and } v_2''(x) + \mu_2 v_2(x) = 0, \tag{1.7}$$

where approximately $\mu_1 \approx \sqrt{3}\pi$ and $\mu_2 \approx \frac{2\pi}{N}$. The mode $v_2(x)$ is the dominant term in the expansion, as seen as comparing $v_2(x)$ with $\sin(\frac{2\pi}{N}x)$ from the unperturbed rectangle. For $v_1(x)$, solving the above with boundary conditions $v_1(0)$ and $v_1(N) = 0$ gives

$$v_1(x) = v_1(0)\left(\cos(\mu_1 x) - \cot(\mu_1 N)\sin(\mu_1 x)\right). \tag{1.8}$$

Moreover, $v(x,y)$ evaluated at the center is given by

$$v\left(\tfrac{N}{2},\tfrac{1}{2}\right) = v_1\left(\tfrac{N}{2}\right) = v_1(0)\left(\cos(\mu_1\tfrac{N}{2}) - \cot(\mu_1 N)\sin(\mu_1\tfrac{N}{2})\right) = \frac{v_1(0)}{2\cos(\mu_1\frac{N}{2})}. \tag{1.9}$$

The term on the right is a periodic function in N with asymptotes where $\mu_1\frac{N}{2} = \frac{\pi}{2} + k\pi$ (or $N \approx \frac{1}{\sqrt{3}} + \frac{2k}{\sqrt{3}}$) for non-negative integer k. We call these the "resonant" values of N since the eigenfunction blows up at the center for such N, and observe that the sign of $v\left(\frac{N}{2},\frac{1}{2}\right)$ changes about these resonant values. Since we are interested in asymptotic results as $N\to\infty$, it will be helpful to work away from these resonant values of N. To this end, we assume throughout this paper that for fixed N,

$$\inf\{|N^* - N| \,:\, \cos(\mu_1\tfrac{N^*}{2}) = 0\} \geq \frac{4}{100\sqrt{3}\pi} > \frac{4}{100\mu_1}, \tag{1.10}$$

since this lets us write explicitly that $\left|2\cos(\mu_1\frac{N}{2})\right|^{-1} \leq 50$.

With this, we are in a position to state our two main theorems.

Theorem 1.1. *Suppose $v_1(0) \neq 0$, $|v_2(0)/v_1(0)| < M$ for some constant M, and that N is away from a resonant value per (1.10). Let d be the distance along the x-axis between the center $(\frac{N}{2}, \frac{1}{2})$ of Ω and the nodal set along either direction $\mathbf{p}_1 = [1, 1]^T$ or $\mathbf{p}_2 = [1, -1]^T$. Then there exists constants C, N_0, and η_0 such that whenever $N \geq N_0$ and $\eta \leq \eta_0$, we have*

$$\left| d - \frac{2}{\left|4\pi v_2'\left(\frac{N}{2}\right) + (\mu_1^2 + \pi^2)v_1\left(\frac{N}{2}\right)\right|} \left(\sqrt{8\pi v_1(\tfrac{N}{2})v_2'(\tfrac{N}{2})} + \frac{1}{2} \frac{\left(v_1'(\frac{N}{2}) - 2\pi v_2(\frac{N}{2})\right)^2 + 2(\mu_1^2 + \pi^2)v_1(\frac{N}{2})^2}{\sqrt{8\pi v_1(\frac{N}{2})v_2'(\frac{N}{2})}} \right) \right|$$

$$\leq C\eta^{3/4}.$$

The constant C depends on N's relative position to resonant value in accordance with (1.10), but is otherwise asymptotically independent of N (and for that matter η). Moreover, future mentions of N_0 and η_0 refer to the same ones stated here.

Estimates on each of the quantities appearing in the expression above let us say that, to leading order, $d = O(\sqrt{\eta})$. This is noteworthy, since it means that the separation distance does not strongly depend on N. If $v_1(0) = 0$, we will see that the term $v_1(x)$ is forced to be identically 0. Thus, looking at (1.5), $v(x, y) = v_2(x)\sin(2\pi y) + E(x, y)$, and any perturbation in the center will be resultant from the higher-order terms. The size of $v_1(0)$ is closely related to the choice of boundary curve ϕ_L, as shown by the following proposition:

Proposition 1.2. *There exists a constant C such that for all $k \geq 0$,*

$$\left| v_k(0) - \frac{4\pi}{N} \int_0^1 \phi_L(y)\sin(2\pi y)\sin(k\pi y)dy \right| \leq C(\eta^{7/4} + k^2\eta^3). \tag{1.11}$$

This proposition is exactly Proposition 5.1 in [1] with a slight adjustment made to correspond to the appropriate mode, and we cite their proof. To see the importance of this proposition, observe that for choices $\phi_L(y)$ that are symmetric about $y = \frac{1}{2}$, the above implies that $v_1(0)$ is small, which has consequences on the scale of the nodal set opening.

Our approach to measuring the nodal set opening consists of Taylor expanding our eigenfunction $v(x, y)$ about the center point $(\frac{N}{2}, \frac{1}{2})$ up to second order, and setting the result equal to 0 to obtain an implicit representation of the nodal set as a hyperbola, written in quadratic form. Once this is done, we choose vectors $\mathbf{p}_1$ and $\mathbf{p}_2$ as directions that closely correspond to the principal axes. In the presence of an opening, one of $\mathbf{p}_1$ and $\mathbf{p}_2$ will intersect the nodal set at exactly two points, one on each branch of the nodal set (while the other passes between the two branches). Therefore, sampling the nodal set along these lines will produce a quadratic in x whose solutions are the $x-$coordinates of the two intersected points. We verify the choice of $\mathbf{p}_1$ and $\mathbf{p}_2$ as close to the principal axes at the end of Section 2.

As hinted at above, the nodal set can be modeled quite well as a hyperbola, reflected in the following theorem.

Theorem 1.3. *There exists $(x_c, y_c) \in \Omega$ and a constant C (asymptotically independent of N) such that when $N \geq N_0$ and $\eta \leq \eta_0$, the nodal set can be written as*

$$\mu_1^2 v_1\left(\tfrac{N}{2}\right)(x - x_c)^2 + 4\pi v_2'\left(\tfrac{N}{2}\right)(x - x_c)(y - y_c) + \pi^2 v_1\left(\tfrac{N}{2}\right)(y - y_c)^2 = 2v\left(\tfrac{N}{2}, \tfrac{1}{2}\right) + \tilde{R}(x, y), \tag{1.12}$$

where

$$|\tilde{R}(x, y)| \leq C\left(\frac{\eta^{3/4}}{N}\right).$$

The coefficients on the left-hand side may be recognized as entries of the Hessian of v calculated at the center point.

To prove these two theorems, we make use of the following proposition, which provides a host of bounds and properties stemming from the decomposition made in (1.5), (1.6):

Proposition 1.4. *There exists constants C (asymptotically independent of N) and c such that when $N \geq N_0$ and $\eta \leq \eta_0$, the following holds:*

(1) $|v_1^{(j)}(x)| \leq C\frac{\eta}{N}$ *for* $0 \leq j \leq 3$ *and* $x \in [0, N]$.

(2) $|v_2^{(j)}(x)| \leq CN^{-j}$ *for* $j = 1, 2$ *and* $x \in [0, N]$.
(3) $C^{-1}N^{-1} \leq |v_2'(x)| \leq CN^{-1}$ *on* $[\frac{2N}{5}, \frac{3N}{5}]$.
(4) *There exists some* $x^* \in (\frac{N}{2} - C\eta, \frac{N}{2} + C\eta)$ *such that* $v_2(x^*) = 0$.
(5) $|v_2(\frac{N}{2})| \leq C\frac{\eta}{N}$.
(6) $\sup_{y\in[0,1]} \left|\nabla^j E(x, y)\right| \leq C\eta e^{-cN}$ *for* $0 \leq j \leq 3$ *and* $x \in [0, N]$.

This proposition is very similar to Prop. 2.1 in [1], and is proved using identical techniques. Proposition 1.4 will be proved in Section 3.

2. Properties of the Nodal Set Opening

In this section we prove Theorems 1.1 and 1.3 assuming Proposition 1.4 holds.

2.1. **Proof of Theorem 1.3.** We begin with the proof of Theorem 1.3, since it follows closely from Taylor expanding $v(x, y)$ about the center $(\frac{N}{2}, \frac{1}{2})$. Doing so, we have

$$v(x,y) = v\left(\tfrac{N}{2}, \tfrac{1}{2}\right) + \nabla v\left(\tfrac{N}{2}, \tfrac{1}{2}\right)\left(x - \tfrac{N}{2}, y - \tfrac{1}{2}\right)^T + \tfrac{1}{2}\left(x - \tfrac{N}{2}, y - \tfrac{1}{2}\right)\mathbf{H}\left(\tfrac{N}{2}, \tfrac{1}{2}\right)\left(x - \tfrac{N}{2}, y - \tfrac{1}{2}\right)^T + R(x,y), \tag{2.1}$$

where

$$\nabla v\left(\tfrac{N}{2}, \tfrac{1}{2}\right) = \begin{pmatrix} v_1'\left(\frac{N}{2}\right) \\ -2\pi v_2\left(\frac{N}{2}\right)\end{pmatrix} + \begin{pmatrix}\partial_x E \\ \partial_y E\end{pmatrix} \tag{2.2}$$

and

$$\mathbf{H}\Big(\frac{N}{2}, \frac{1}{2}\Big) = \begin{pmatrix} -\mu_1^2 v_1\left(\frac{N}{2}\right) & -2\pi v_2'\left(\frac{N}{2}\right) \\ -2\pi v_2'\left(\frac{N}{2}\right) & -\pi^2 v_1\left(\frac{N}{2}\right)\end{pmatrix} + \begin{pmatrix}\partial_{xx}E & \partial_{xy}E \\ \partial_{xy}E & \partial_{yy}E\end{pmatrix}, \tag{2.3}$$

where all the partial derivatives in E are evaluated at $\left(\frac{N}{2}, \frac{1}{2}\right)$ whenever they are written without an argument.

We restrict the expansion to a neighborhood U about the center of radius $C\eta^{1/4}$. This radius is chosen to capture important pieces of the nodal set while keeping the remainder term small. On this neighborhood, we have the following uniform bound on the remainder term.

Lemma 2.1. *There exists a constant* C *(asymptotically independent of* N*) such that if* $N \geq N_0$ *and* $\eta \leq \eta_0$ *then*

$$\sup_{(x,y)\in U} |R(x,y)| \leq C\left(\frac{\eta^{3/4}}{N}\right). \tag{2.4}$$

Proof. The remainder term can be written in multi-index notation, where $\alpha = (\alpha_1, \alpha_2)$, as

$$R(x,y) = \sum_{|\alpha|=3} \frac{1}{\alpha!} v^{(\alpha)}(P_\theta)(x - \tfrac{N}{2})^{\alpha_1}(y - \tfrac{1}{2})^{\alpha_2}$$

where $P_\theta = \left(\frac{N}{2} + \theta(x - \frac{N}{2}), \frac{1}{2} + \theta(x - \frac{N}{2})\right)$, for some $\theta \in [0, 1]$. Thus, for $(x, y) \in U$, we have the estimate that

$$|R(x,y)| \leq C \sup_{\substack{(x,y)\in U \\ |\alpha|=3}} |v^{(\alpha)}(x,y)|\eta^{3/4}.$$

(We have dropped θ dependence by way of taking the supremum over U.) We compute the bound for $\alpha = (0, 3)$, i.e. the term $\partial_y^3 v(x, y)$, for the sake of demonstration - the bounds for the other three terms, though slightly different, follow similarly. From (1.5) we have

$$|\partial_y^3 v(x,y)| \leq \pi^3 |v_1(x)\cos(\pi y)| + 8\pi^3 |v_2(x)\cos(2\pi y)| + |\partial_y^3 E(x,y)|.$$

Write $y = \frac{1}{2} + \varepsilon$ for $|\varepsilon| \leq C\eta^{1/4}$. Thus, $|\cos(\pi y)| = |\sin(\pi\varepsilon)| \leq C\eta^{1/4}$. Otherwise $|\cos(2\pi y)| \leq 1$, and for $v_2(x)$, write

$$|v_2(x)| \leq |v_2(\tfrac{N}{2})| + \left|x - \tfrac{N}{2}\right| \sup_{|x - \frac{N}{2}| \leq C\eta^{1/4}} |v_2'(x)|.$$

Prop. 1.4, parts (3) and (5), then imply that

$$|v_2(x)| \leq C\left(\frac{\eta}{N}\right) + C\left(\frac{\eta^{1/4}}{N}\right).$$

Combining the above with Prop. 1.4, parts (1) and (6), gives

$$|\partial_y^3 v(x,y)| \leq C\left(\frac{\eta^{5/4}}{N}\right) + C\left(\frac{\eta}{N}\right) + C\left(\frac{\eta^{1/4}}{N}\right) + C\eta e^{-cN}. \tag{2.5}$$

Similarly, across all $|\alpha| = 3$ we can collect terms and write

$$\sup_{\substack{(x,y)\in U \\ |\alpha|=3}} |v^{(\alpha)}(x,y)| \leq C\left[\frac{\eta^{5/4}}{N} + \frac{\eta}{N} + \frac{\eta^{1/4}}{N} + N^{-2} + N^{-3}\eta^{1/4} + \eta e^{-cN}\right] \leq CN^{-1}$$

for $\eta < 1/2$ sufficiently small, $N > 1$ sufficiently large, and some new constant C. To comment on where the new terms since (2.5) came from, the $N^{-3}\eta^{1/4}$ term comes from bounding $v_2'''(x)\sin(2\pi y)$ from $\partial_x^3 v(x,y)$, and the N^{-2} term comes from bounding $v_2''(x)\cos(2\pi y)$ in $\partial_x^2\partial_y v(x,y)$. The lemma thus follows. □

We proceed with the proof of Theorem 1.3. Set $p = (x - \frac{N}{2})$, $q = (y - \frac{1}{2})$, and $\mathbf{H} := \mathbf{H}\left(\frac{N}{2}, \frac{1}{2}\right)$ for ease of notation. We expand (2.1) using (2.2) and (2.3) and write

$$\begin{aligned} v(x,y) &= \frac{1}{2}\Big[-\mu_1^2 v_1\left(\tfrac{N}{2}\right)p^2 - 4\pi v_2'\left(\tfrac{N}{2}\right)pq - \pi^2 v_1\left(\tfrac{N}{2}\right)q^2 + 2v_1'\left(\tfrac{N}{2}\right)p - 4\pi v_2\left(\tfrac{N}{2}\right)q + 2\left(v\left(\tfrac{N}{2},\tfrac{1}{2}\right) + R(x,y)\right)\Big] \\ &= \frac{1}{2}\big[\alpha p^2 + 2\gamma pq + \beta q^2 + 2ap + 2bq + c\big], \text{ matching coefficients} \\ &= 0. \end{aligned}$$

The above quadratic form will describe a hyperbola provided $\begin{vmatrix}\alpha & \gamma \\ \gamma & \beta\end{vmatrix} = \det\mathbf{H} < 0$. This holds when $4\pi^2(v_2'\left(\frac{N}{2}\right))^2 > \mu_1^2\pi^2(v_1\left(\frac{N}{2}\right))^2$ which per Prop. 1.4 holds for η sufficiently small.

Moreover, we have the following lower bound

$$\begin{aligned} |\det\mathbf{H}| &\geq \left|2\pi v_2'\left(\tfrac{N}{2}\right)^2 - \mu_1^2\pi^2 v_1\left(\tfrac{N}{2}\right)^2\right| \\ &\geq C^{-2}N^{-2} - C\left(\tfrac{\eta}{N}\right)^2 \\ &\geq CN^{-2} \end{aligned}$$

for η sufficiently small and for some new constant C.

Using a change of coordinates to recenter about the hyperbola's center, (x_c, y_c), and reverting back to (x,y) coordinates, we may write the hyperbola as

$$\mu_1^2 v_1\left(\tfrac{N}{2}\right)(x-x_c)^2 + 4\pi v_2'\left(\tfrac{N}{2}\right)(x-x_c)(y-y_c) + \pi^2 v_1\left(\tfrac{N}{2}\right)(y-y_c)^2 = \frac{D}{\det\mathbf{H}}, \tag{2.6}$$

where

$$D = \begin{vmatrix}\alpha & \gamma & a \\ \gamma & \beta & b \\ a & b & c\end{vmatrix} = -(\alpha b^2 + \beta a^2) + 2ab\gamma + c\det\mathbf{H}.$$

The sign of

$$\begin{aligned} \frac{D}{\det\mathbf{H}} &= \frac{\alpha b^2 + \beta a^2}{\det\mathbf{H}} - \frac{2ab\gamma}{\det\mathbf{H}} + c \\ &= \frac{\alpha b^2 + \beta a^2}{\det\mathbf{H}} - \frac{2ab\gamma}{\det\mathbf{H}} + 2\left(v\left(\tfrac{N}{2},\tfrac{1}{2}\right) + R(x,y)\right) \end{aligned}$$

determines the orientation of the opening - were the sign to change, the nodal set would switch to the conjugate hyperbola. Using the lower bound on $\det \mathbf{H}$ and bounds in Prop. 1.4, we have

$$\left|\frac{\alpha b^2+\beta a^2}{\det \mathbf{H}}\right| \leq C\left(\frac{\eta^3}{N}\right) \text{ and } \left|\frac{ab\gamma}{\det \mathbf{H}}\right| \leq C\left(\frac{\eta^2}{N}\right).$$

Lastly, set $\tilde{R}(x,y) = 2R(x,y) + \frac{\alpha b^2+\beta a^2}{\det \mathbf{H}} - \frac{2ab\gamma}{\det \mathbf{H}}$, and the bounds on $|\tilde{R}(x,y)|$ follow from Lemma 2.1, the bounds directly above, and the fact that $\eta < 1/2$. □

The bound on the remainder lets us view $v\left(\frac{N}{2},\frac{1}{2}\right)$ as the dominant term on the right side of (1.12), being of size $O(\frac{\eta}{N})$, and the one that determines the orientation of the hyperbola.

2.2. **Proof of Theorem 1.1.** We turn to estimating the length of the nodal set gap. As mentioned, we sample the nodal set along appropriate diagonals to produce a quadratic in x, and we do this instead of reading off the separation distance directly from the hyperbola model. The reason for this is the latter requires a precise understanding of the eigenvalues of $\mathbf{H}(\frac{N}{2},\frac{1}{2})$, which are difficult to compute exactly. We ignore the remainder term in calculating the roots, and argue later that including it as a constant term does not notably alter the roots.

As earlier, write $\mathbf{H} := \mathbf{H}\left(\frac{N}{2},\frac{1}{2}\right)$ for ease. Taking $\mathbf{p} = (x-\frac{N}{2})[1,\pm 1]^T = (x-\frac{N}{2})\mathbf{p'}$, where the $\pm$ depends on which diagonal is chosen, we have from the Taylor expansion (2.1) that

$$\begin{aligned} 0 &= v\left(\tfrac{N}{2},\tfrac{1}{2}\right) + \nabla v\left(\tfrac{N}{2},\tfrac{1}{2}\right)\cdot \mathbf{p} + \tfrac{1}{2}\mathbf{p}^T\mathbf{H}\mathbf{p} \\ &= v\left(\tfrac{N}{2},\tfrac{1}{2}\right) + (x-\tfrac{N}{2})\left(\nabla v\left(\tfrac{N}{2},\tfrac{1}{2}\right)\cdot \mathbf{p'}\right) + (x-\tfrac{N}{2})^2\left(\tfrac{1}{2}\mathbf{p'}^T\mathbf{H}\mathbf{p'}\right). \end{aligned} \tag{2.7}$$

The solution for x is thus given by

$$\hat{x} = \frac{N}{2} - \frac{\nabla v(\frac{N}{2},\frac{1}{2})\cdot \mathbf{p'}}{\mathbf{p'}^T\mathbf{H}\mathbf{p'}} \pm \frac{\sqrt{\left(\nabla v(\frac{N}{2},\frac{1}{2})\cdot \mathbf{p'}\right)^2 - 2v(\frac{N}{2},\frac{1}{2})\left(\mathbf{p'}^T\mathbf{H}\mathbf{p'}\right)}}{\mathbf{p'}^T\mathbf{H}\mathbf{p'}}.$$

The key term to focus on is the discriminant,

$$\Delta := \left(\nabla v\left(\tfrac{N}{2},\tfrac{1}{2}\right)\mathbf{p'}\right)^2 - 2v\left(\tfrac{N}{2},\tfrac{1}{2}\right)\left(\mathbf{p'}^T\mathbf{H}\left(\tfrac{N}{2},\tfrac{1}{2}\right)\mathbf{p'}\right). \tag{2.8}$$

The separation between the two nodal sets along the x-axis is $2\sqrt{\Delta}/\left|\mathbf{p'}^T\mathbf{H}\mathbf{p'}\right|$. Moreover, if for a particular diagonal we have $\Delta < 0$, then there is no real solution in x, and so that diagonal must pass between the two nodal sets.

Substituting $\mathbf{p'} = [1,\pm 1]^T$, and setting $v\left(\frac{N}{2},\frac{1}{2}\right) = v_1(\frac{N}{2})$ while we are paused, we obtain

$$\Delta = \left(v_1'\left(\frac{N}{2}\right) \mp 2\pi v_2\left(\frac{N}{2}\right)\right)^2 + 2v_1\left(\frac{N}{2}\right)\left[(\mu_1^2+\pi^2)v_1\left(\frac{N}{2}\right) \pm 4\pi v_2'\left(\frac{N}{2}\right)\right]. \tag{2.9}$$

We seek expressions for $\sqrt{\Delta}$. Rewrite Δ as

$$\Delta = \underbrace{\left(v_1'\left(\frac{N}{2}\right) \mp 2\pi v_2\left(\frac{N}{2}\right)\right)^2}_{:=A^2} + \underbrace{2(\mu_1^2+\pi^2)v_1\left(\frac{N}{2}\right)^2}_{:=B} \pm \underbrace{8\pi v_1\left(\frac{N}{2}\right)v_2'\left(\frac{N}{2}\right)}_{:=\Gamma}.$$

Since $v_1(\frac{N}{2}) \neq 0$, then B is strictly positive. Write $X^2 := A^2 + B > 0$. Therefore, we can write

$$\Delta = X^2 \pm \Gamma = \Gamma\left(1 \pm \frac{X^2}{\Gamma}\right), \tag{2.10}$$

$$\text{or in other words, } \sqrt{\Delta} = \sqrt{\Gamma}\sqrt{1 \pm \frac{X^2}{\Gamma}}, \tag{2.11}$$

where the choice of plus or minus depends on which diagonal we are on. The term Γ may be of either sign, but due to the presence of the plus or minus we may take $\Gamma > 0$ without loss. Note though that $\Gamma \neq 0$ since $v_2'(\frac{N}{2}) \neq 0$.

We recall that, since the sampling directions correspond to the principal axes of the hyperbolas, only one of them will intersect both branches of the hyperbola while the other will pass between them. Therefore, for some choice of diagonal, we expect imaginary solutions. For $\Gamma > 0$, this corresponds exactly to the choice of "$-$" in (2.10): We would have $X^2 + \Gamma > X^2 - \Gamma$, and since one of these terms must be negative we must have $\Delta = X^2 - \Gamma < 0$. This is also consistent when viewing $X^2 = O(\frac{\eta^2}{N^2})$ compared to $\Gamma = O(\frac{\eta}{N^2})$. Thus, we can assume that $\sqrt{\Delta} = \Gamma\sqrt{1 + \frac{X^2}{\Gamma}}$. One small detail is that this fixes the choice of sign in the expression A^2 above to be negative (i.e., the choice of $\mathbf{p}' = [1,\ 1]^T$).

Taylor expanding $\sqrt{1+x}$ about $x = 0$ with remainder, we have that

$$\sqrt{1 + \frac{X^2}{\Gamma}} = 1 + \frac{1}{2}\frac{X^2}{\Gamma} - \frac{1}{8}(1+\xi)^{-3/2}\frac{X^4}{\Gamma^2}.$$

for some $\xi \in (0, \frac{B}{A^2})$. We wish to consider the right-most term as an error term, denoted E. To do this, we start by bounding it. Over the interval $(0, \frac{X^4}{\Gamma^2})$, the largest value $(1+\xi)^{-3/2}$ can take is 1 for $\xi = 0$. We can then write

$$|E| \leq \frac{1}{8}\frac{X^4}{\Gamma^2}.$$

With this, we obtain:

$$\sqrt{\Delta} = \Gamma^{1/2} + \frac{1}{2}X^2\Gamma^{-1/2} + E', \text{ where} \tag{2.12}$$

$$X^2 = A^2 + B = \left(v_1'(\frac{N}{2}) - 2\pi v_2(\frac{N}{2})\right)^2 + 2(\mu_1^2 + \pi^2)v_1(\frac{N}{2})^2, \tag{2.13}$$

$$\Gamma = 8\pi v_1(\frac{N}{2})v_2'(\frac{N}{2}), \tag{2.14}$$

$$E' = \Gamma^{1/2} \cdot E \leq \frac{1}{8}\frac{X^4}{\Gamma^{3/2}}. \tag{2.15}$$

It remains to bound $\frac{X^4}{\Gamma^{3/2}}$. To start, write

$$\begin{aligned}\frac{X^4}{\Gamma^{3/2}} &= \frac{(A^2+B)^4}{\Gamma^{3/2}} \\ &= (A^2+B)^{5/2}\left[\frac{A^2}{\Gamma} + \frac{B}{\Gamma}\right]^{3/2}.\end{aligned} \tag{2.16}$$

From (2.13) and earlier bounds in Prop. 1.4 we have $|A^2 + B| \leq C\frac{\eta^2}{N^2}$. We consider the two terms in the brackets, beginning with $\frac{B}{\Gamma}$, which we can write as

$$\begin{aligned}\frac{B}{\Gamma} &= \frac{2(\mu_1^2+\pi^2)v_1(\frac{N}{2})^2}{8\pi v_1(\frac{N}{2})v_2'(\frac{N}{2})} \\ &= \frac{2(\mu_1^2+\pi^2)v_1(\frac{N}{2})}{8\pi v_2'(\frac{N}{2})}.\end{aligned}$$

But $v_2'(\frac{N}{2}) \geq C^{-1}N^{-1}$ and $v_1(\frac{N}{2}) \leq C\eta N^{-1}$, and so $\frac{B}{\Gamma} \leq C\eta$.

Moving to $\frac{A^2}{\Gamma}$, we write

$$\begin{aligned}\frac{A^2}{\Gamma} &= \frac{\left(v_1'(\frac{N}{2}) - 2\pi v_2(\frac{N}{2})\right)^2}{8\pi v_1(\frac{N}{2})v_2'(\frac{N}{2})} \\ &= \frac{v_1'(\frac{N}{2})^2}{8\pi v_1(\frac{N}{2})v_2'(\frac{N}{2})} + \frac{4\pi^2 v_2(\frac{N}{2})^2}{8\pi v_1(\frac{N}{2})v_2'(\frac{N}{2})} - \frac{4\pi v_1'(\frac{N}{2})v_2(\frac{N}{2})}{8\pi v_1(\frac{N}{2})v_2'(\frac{N}{2})}.\end{aligned}$$

Notice that in the first and third terms, the ratio $\frac{v_1'(\frac{N}{2})}{v_1(\frac{N}{2})} = -\tan(\mu_1 \frac{N}{2})$ by definition of $v_1(x)$. So, working away from the resonant N under assumption (1.10),

$$\frac{v_1'(\frac{N}{2})^2}{8\pi v_1(\frac{N}{2}) v_2'(\frac{N}{2})} = -\frac{\mu_1^2}{8\pi}\tan(\mu_1 \tfrac{N}{2})\frac{v_1'(\frac{N}{2})}{v_2'(\frac{N}{2})} \leq C\eta$$

and

$$\frac{4\pi v_1'(\frac{N}{2}) v_2(\frac{N}{2})}{8\pi v_1(\frac{N}{2}) v_2'(\frac{N}{2})} = \frac{\mu_1}{2}\tan(\mu_1 \tfrac{N}{2})\frac{v_2(\frac{N}{2})}{v_2'(\frac{N}{2})} \leq C\eta.$$

In the above, the constant C changes from line to line, and depends on N's distance from a resonant value in accordance with (1.10). We have also again made use of the lower bound on $v_2'(\frac{N}{2})$ and upper bounds on $v_1'(\frac{N}{2})$ and $v_2(\frac{N}{2})$.

We consider the second term now. Since by assumption the ratio $|\frac{v_2(0)}{v_1(0)}| \leq M$ for some constant M, we can say

$$\begin{aligned}\frac{4\pi^2 v_2(\frac{N}{2})^2}{8\pi v_1(\frac{N}{2}) v_2'(\frac{N}{2})} &= \frac{4\pi^2 v_2(0)\cos(\mu_2 \frac{N}{2}) v_2(\frac{N}{2})}{8\pi v_1(0)\cos(\mu_1 \frac{N}{2}) v_2'(\frac{N}{2})} \\ &= \frac{\pi}{2}\frac{v_2(0)}{v_1(0)}\frac{\cos(\mu_2 \frac{N}{2}) v_2(\frac{N}{2})}{\cos(\mu_1 \frac{N}{2}) v_2'(\frac{N}{2})} \\ &\leq M \cdot C\eta.\end{aligned}$$

Picking back up from (2.16) and applying these bounds, we have

$$\begin{aligned}\frac{X^4}{\Gamma^{3/2}} &= (A^2+B)^{5/2}\big[\frac{A^2}{\Gamma} + \frac{B}{\Gamma}\big]^{3/2} \\ &\leq C(\frac{\eta^2}{N^2})^{5/2}\big[\eta\big]^{3/2} \\ &= C\frac{\eta^{13/2}}{N^5}.\end{aligned}$$

Overall then, we obtain

$$\sqrt{\Delta} = \sqrt{8\pi v_1(\frac{N}{2}) v_2'(\frac{N}{2})} + \frac{1}{2}\frac{\left(v_1'(\frac{N}{2}) - 2\pi v_2(\frac{N}{2})\right)^2 + 2(\mu_1^2+\pi^2) v_1(\frac{N}{2})^2}{\sqrt{8\pi v_1(\frac{N}{2}) v_2'(\frac{N}{2})}} + \text{Error}, \tag{2.17}$$

$$\text{where } |\text{Error}| \leq C\frac{\eta^{13/2}}{N^5}. \tag{2.18}$$

To conclude, we multiply by $2/|\mathbf{p'Hp'}|$ to get the separation distance. Recall from earlier that our assumptions on the sign of Γ forced $\mathbf{p'} = [1,\, 1]^T$. Therefore,

$$\begin{aligned}|\mathbf{p'Hp'}| &= \left|4\pi v_2'\left(\tfrac{N}{2}\right) + (\mu_1^2+\pi^2) v_1\left(\tfrac{N}{2}\right)\right| \\ &\geq \left|4\pi v_2'\left(\tfrac{N}{2}\right)\right| - (\mu_1^2+\pi^2)\left|v_1\left(\tfrac{N}{2}\right)\right| \\ &\geq CN^{-1}\end{aligned}$$

for η sufficiently small and some new constant C. The Error term therefore becomes $O(\frac{\eta^{13/2}}{N^4})$.

Accounting for the remainder term $R(x,y)$ now, we see that above estimate still holds, but now for larger error.

Lemma 2.2. *Let r_1 and r_2 be distinct solutions to (2.7), and suppose that*

$$\min\{|r_1 - \tfrac{N}{2}|, |r_2 - \tfrac{N}{2}|\} \geq \varepsilon > 0$$

for some constant ε. Then there exists a constant C such that when $N \geq N_0$ and $\eta \leq \eta_0$, adding $R(x,y)$ to (2.7) will shift the roots by $C\eta^{3/4}$ at most.

Proof. The proof is an application of Implicit Function Theorem, following, e.g., [4]. Set $f(a,b,c,x) = ax^2+bx+c$, and note $f\left(\frac{1}{2}\mathbf{p'}^T\mathbf{H}\mathbf{p'}, \nabla v\left(\frac{N}{2},\frac{1}{2}\right)\cdot\mathbf{p'}, v\left(\frac{N}{2},\frac{1}{2}\right), r_1-\frac{N}{2}\right)=0$. Moreover, we may write

$$\begin{aligned}\left|\partial_x f\left(\tfrac{1}{2}\mathbf{p'}^T\mathbf{H}\mathbf{p'}, \nabla v\left(\tfrac{N}{2},\tfrac{1}{2}\right)\cdot\mathbf{p'}, v\left(\tfrac{N}{2},\tfrac{1}{2}\right), r_1-\tfrac{N}{2}\right)\right| &= \left|\mathbf{p'}^T\mathbf{H}\mathbf{p'}(r_1-\tfrac{N}{2}) + \nabla v\left(\tfrac{N}{2},\tfrac{1}{2}\right)\cdot\mathbf{p'}\right| \\ &\geq \left|\varepsilon\mathbf{p'}^T\mathbf{H}\mathbf{p'}\right| - \left|\nabla v\left(\tfrac{N}{2},\tfrac{1}{2}\right)\cdot\mathbf{p'}\right|.\end{aligned}$$

Reusing the bound on $|\mathbf{p'}\mathbf{H}\mathbf{p'}|$ from the proof of Theorem 1.1 as well as bounds on the entries of $\nabla v\left(\frac{N}{2},\frac{1}{2}\right)$ from Prop. 1.4, we have that

$$\left|\partial_x f\left(\tfrac{1}{2}\mathbf{p'}^T\mathbf{H}\mathbf{p'}, \nabla v\left(\tfrac{N}{2},\tfrac{1}{2}\right)\cdot\mathbf{p'}, v\left(\tfrac{N}{2},\tfrac{1}{2}\right), r_1-\tfrac{N}{2}\right)\right| \geq CN^{-1}. \tag{2.19}$$

Therefore, there exists a graph function $g(a,b,c)$ and a neighborhood U about the above point such that $f^{-1}(0)\cap U = \{(a,b,c,x) : x = g(a,b,c)\}$, and moreover,

$$\partial_c g(a,b,c) = -\frac{\partial_c f(a,b,c,x)}{\partial_x f(a,b,c,x)}.$$

Since $\partial_c f(a,b,c,x) = 1$, then (2.19) implies $|\partial_c g(a,b,c)| < CN$. Therefore, when $R(x,y)$ is included as a constant in (2.7), the root r_1 moves by a distance at most

$$C|R(x,y)|N \leq C\eta^{3/4}$$

by Lemma 2.1. The same holds for r_2, and this yields the claim. □

In Theorem 1.1, we claimed that the best directions to sample along were $\mathbf{p}_1 = [1,\,1]^T$ or $\mathbf{p}_2 = [1,\,-1]^T$. The following verifies that choice.

Proposition 2.3. *Let $\varphi = \varphi(N)$ be the angle the principal axis makes with the x-axis. Then there exists a constant $\tilde{C}$ such that when $N \geq N_0$ and $\eta \leq \eta_0$ then $\left||\varphi| - \frac{\pi}{4}\right| \leq \tilde{C}\eta$.*

Proof. From (2.3), the angle φ satisfies

$$\tan(2\varphi) = \frac{2\left(-2\pi v_2'\left(\frac{N}{2}\right) + \partial_{xy}E\right)}{-\left(\mu_1^2+\pi^2\right)v_1\left(\frac{N}{2}\right) + \partial_{xx}E + \partial_{yy}E}.$$

From Proposition 1.4 we have the lower bound $C^{-1}N^{-1} \leq |v_2'(\frac{N}{2})|$ and the upper bound $|v_1(\frac{N}{2})| \leq C\frac{\eta}{N}$. Moreover, we have the crude bounds, provided $\eta < 1$ and $N > 1$, that

$$C\eta e^{-cN} \leq C_1\eta N^{-1} \leq C_1 N^{-1}$$

for some constant C_1. This gives

$$\begin{aligned}\left|2\left(-2\pi v_2'\left(\tfrac{N}{2}\right) + \partial_{xy}E\right)\right| &\geq |4\pi v_2'(\tfrac{N}{2})| - 2C_1N^{-1} \\ &\geq C_2N^{-1}\end{aligned}$$

and

$$\begin{aligned}\left|-\left(\mu_1^2+\pi^2\right)v_1\left(\tfrac{N}{2}\right) + \partial_{xx}E + \partial_{yy}E\right| &\leq C\tfrac{\eta}{N} + 2C\eta e^{-cN} \\ &\leq C_3\eta N^{-1}.\end{aligned}$$

Therefore, we can bound $|\tan(2\varphi)|$ from below as

$$|\tan(2\varphi)| \geq \frac{C_2N^{-1}}{C_3\eta N^{-1}} = \frac{C'}{\eta}.$$

This yields $\frac{C'}{\eta} \leq |\tan(2\varphi)| \leq \infty$. Take $\varphi > 0$ without loss (the case $\varphi < 0$ follows similarly with minor modifications), and since tangent is monotonic on $[-\frac{\pi}{2},\frac{\pi}{2}]$, we obtain

$$\arctan\left(\frac{C'}{\eta}\right) \leq 2\varphi \leq \frac{\pi}{2}.$$

Write $\arctan\left(\frac{C'}{\eta}\right) = \frac{\pi}{2} - \xi$ for some $\xi \geq 0$. Manipulation then yields

$$\left|\varphi - \frac{\pi}{4}\right| \leq \frac{\xi}{2}.$$

It remains to bound ξ. To do this, note that

$$\frac{C'}{\eta} = \tan\left(\frac{\pi}{2} - \xi\right) = \frac{1}{\tan(\xi)}$$

and therefore

$$\xi = \arctan\left(\frac{\eta}{C'}\right) \leq \frac{\eta}{C'}.$$

And so,

$$\left|\varphi - \frac{\pi}{4}\right| \leq \frac{\eta}{2C'} := \tilde{C}\eta.$$

Doing the same with $\varphi < 0$ yields the claim. □

3. Proof of Proposition 1.4

In this section, we prove Proposition 1.4 using the properties of the domain and our eigenfunction decomposition. Proposition 1.4 is analogous to Prop. 2.1 in [1], and our method of proof directly follows theirs: In fact, Lemmas 3.1 - 3.3 here mirror Lemmas 4.1 - 4.3 of [1] respectively.

Lemma 3.1. *The eigenvalue μ, where $\Delta v + \mu v = 0$, satisfies*

$$4\pi^2\left(\tfrac{1}{N^2} + 1\right) \geq \mu \geq 4\pi^2\left(\tfrac{1}{(N+\eta)^2} + 1\right). \tag{3.1}$$

Proof. We observe that

$$[0, N] \times [0, 1] \subset \Omega \subset [-\eta, N] \times [0, 1]$$

and apply domain monotonicity for Dirichlet eigenvalues to obtain the claim. □

The above eigenvalue bound yields the following estimates on the size of v away from the boundary.

Lemma 3.2. *There exists a constant C such that $|\nabla v(x, y)| \leq C$. Further, letting $d(x) = \min\{x, N-x\}$, we have $|v(x, y)| \leq CN^{-1}(\eta + d(x))$.*

Proof. We follow the proof of Lemma 4.2 in [1]. The bound on $|\nabla v(x, y)|$ follows from the fact that the boundary of Ω is C^2-smooth, save for four points where the side curves meet at convex angles. For the remaining point-wise bound, define the comparison function

$$S(x, y) = C_1 \sin\left(2\pi\frac{x+\eta}{c_1 N}\right)\sin(2\pi y)$$

where $c_1 > 0$ is chosen to ensure $(\Delta + \mu)S < 0$ for $x \leq c_1\frac{N}{2} - \eta$. (For instance, compute S's eigenvalue explicitly and write it as $\mu + \varepsilon(c_1, N)$, where the difference $\varepsilon(c_1, N)$ depends on c_1 and N, and then choose c_1 appropriately to ensure $\varepsilon(c_1, N) > 0$.) Since $v = 0$ on $\partial\Omega$ and the gradient is bounded, the constant C_1 can be chosen large enough to give $|v(x, y)| \leq S(x, y)$ for $(x, y) \in \Omega$ on line $x = c_1\frac{N}{2} - \eta$. We can then apply a generalized maximum principle (see Theorem A.1 of [6]) to get

$$|v(x, y)| \leq S(x, y) \leq C\tfrac{x+\eta}{N} \text{ on } \{(x, y) \in \Omega : x \leq c_1\tfrac{N}{2} - \eta\}.$$

This gives the bound for $x \leq \frac{N}{2}$. In the case for $x \geq \frac{N}{2}$, the above argument can be simplified by setting $\eta := 0$ due to the flat right side. □

To prove Proposition 1.4, we proceed to specify a system of ODEs describing the modes arising in our eigenvalue decomposition. Recall from (1.4-5) that

$$v(x, y) = \sum_{k\geq 1} v_k(x)\sin(2\pi y)$$

where

$$v_k(x) = 2\int_0^1 v(x,y)\sin(k\pi y).$$

We can specify estimates at the boundary points $v_k(0)$ and $v_k(N)$ for each mode.

Lemma 3.3. *There exists a constant C such that $|v_k(0)| \leq C\frac{\eta}{N}$ for all k. Moreover, $v_k(N) = 0$ for all k.*

Proof. From Lemma 3.2, we see that $|v(0,y)| \leq C\frac{\eta}{N}$. Therefore we immediately have

$$|v_k(0)| = \left|2\int_0^1 v(0,y)\sin(k\pi y)\right| \leq C\frac{\eta}{N}$$

for a new constant C. Writing out a similar integral for $v_k(N)$, we see that $v_k(N) = 0$ since the Dirichlet boundary conditions force $v(N,y) \equiv 0$. □

Proof of Proposition 1.4: From $(\Delta + \mu)v = 0$ for $x \in [0,N]$ and $v = \sum_k v_k(x)\sin(k\pi y)$, we see that each v_k obeys

$$v_k'' + (\mu - \pi^2 k^2)v_k = 0. \tag{3.2}$$

We use this system to obtain parts (1) - (6) of Proposition 1.4.

Let $\mu_k^2 := \pi^2 k^2 - \mu$, and observe by the eigenvalue bounds (3.1) that $\mu_k^2 \geq 0$ for $k \geq 3$. Therefore, for all modes with $k \geq 3$, we have that

$$v_k(x) = \frac{1}{\sinh(\mu_k N)} v_k(0)\sinh\left(\mu_k(N-x)\right).$$

Recalling that $E(x,y) = \sum_{k\geq 3} v_k(x)\sin(2\pi y)$, the above yields the bounds on the error term stated in part (6) for Proposition 1.4.

We now consider the $k = 1, 2$ modes and obtain the remaining estimates.

For $k = 1$, we similarly have

$$\frac{4\pi^2}{(N+2\eta)^2} + 3\pi^2 \leq \mu - \pi^2 \leq \frac{4\pi^2}{N^2} + 3\pi^2.$$

Letting $\mu_1^2 = \mu - \pi^2$, we have then that $\mu_1^2 > 0$ by the above. Hence, solving for $v_1(x)$ gives

$$v_1(x) = v_1(0)\cos(\mu_1 x) + B_1\sin(\mu_1 x), \tag{3.3}$$

$$\text{where } B_1 = \frac{-v_1(0)\cos(\mu_1 N)}{\sin(\mu_1 N)}. \tag{3.4}$$

The denominator, $\sin(\mu_1 N)$, will not generally vanish in line with the hypothesis from (1.10) that N is bounded away from resonant values. Therefore, we have that $|B_1| \leq C\frac{\eta}{N}$, and we accordingly obtain part (1) of Proposition 1.4.

When $k = 2$, we have from (3.1),

$$\frac{4\pi^2}{(N+2\eta)^2} \leq \mu - 4\pi^2 \leq \frac{4\pi^2}{N^2}.$$

Let $\mu_2^2 = \mu - 4\pi^2 > 0$. Solving for $v_2(x)$ gives

$$v_2(x) = v_2(0)\cos(\mu_2 x) + A_1\sin(\mu_2 x), \tag{3.5}$$

$$\text{where } A_1 = \frac{-v_2(0)\cos(\mu_2 N)}{\sin(\mu_2 N)}. \tag{3.6}$$

Since $\mu_2 \approx \frac{2\pi}{N}$, we need a bit of care in controlling A_1. We can write

$$|v_2(x) - A_1\sin(\mu_2 x)| = |v_2(0)\cos(\mu_2 x)| \leq C\frac{\eta}{N}$$

using Lemma 4.3. Then, applying the reverse triangle inequality to $|v_2(x) - A_1\sin(\mu_2 x)|$ and using $\|v\|_{L^\infty} = 1$ gives $||A_1| - 1| \leq C\frac{\eta}{N}$.

With the above in hand, we can prove parts (2-5) of Proposition 1.4. For part (2), observe that $\mu_2 \leq \frac{2\pi}{N}$. Therefore, since derivatives of v_2 contain powers of μ_2, we have readily that $v_2^{(j)}(x) \leq CN^{-j}$ for some constant C and $j = 1, 2$.

From differentiating $v_2(x)$ we see that $|v_2'(x) - A_1\mu_2 \cos(\mu_2 x)| \leq C\frac{\eta}{N}$. Using the bound on A_1 and the eigenvalue bound gives that $C^{-1}N^{-1} \leq |v_2'(x)|$ on $[\frac{2N}{5}, \frac{3N}{5}]$ for η sufficiently small. This yields part (3). Proving part (4) takes directly after Prop. 4.3 in [1]. Since $|v_2'(x)|$ is strictly positive, we are guaranteed at most one zero in $[\frac{2N}{5}, \frac{3N}{5}]$. Further since $|v_2(x) - A_1 \sin(\mu_2 x)| \leq C\frac{\eta}{N}$ and since $\sin(\mu_2 x)$ vanishes somewhere near $x = N/2$, we get a bounding interval for the zero of v_2, namely that $v_2(x) = 0$ for some $x^* \in [\frac{N}{2} - C\eta, \frac{N}{2} + C\eta]$ for constant C.

Further, using the above x^* where $v_2(x^*) = 0$, we integrate away from this zero to the center to get $\left|v_2(\frac{N}{2})\right| = \left|\int_{x^*}^{N/2} v_2'(x)\right| \leq C\frac{\eta}{N}$, which is precisely part (5) of Proposition 1.4.

4. Numerical Experiments

In this section we detail numerical experiments that investigate our findings. We consider a few different classes of boundary functions, namely sinusoids (even and odd about $y = \frac{1}{2}$), as well as some irregular boundary functions including hats and (non-smooth) bumps. To this last point, we relax the assumption that $\phi_L \in C^2([0,1];\mathbb{R})$ and require it to only be (Lipschitz) continuous. We also loosen the perturbation bound and let $\phi_L(y) \in [-\eta, \eta]$ rather than $[-\eta, 0]$. Consequently, we also allow for $\phi_L(0), \phi_L(1) \neq 0$.

We begin with a brief description of the numerical methods, and then explore three of our findings, namely that symmetry in the boundary perturbation can close the nodal set, that the nodal set switches orientation about the described resonant N, and that the nodal set gap distance is independent of N. The numerics provide good support for these findings.

4.1. Description of Numerical Methods.

The analysis was performed using MATLAB, which provides tools for solving PDEs on user-defined domains. Domains were specified using `polyshape` in MATLAB, which accepts coordinate vectors as an argument and returns a polygon-geometry object. To encode the left boundary perturbation, the interval $[0, 1]$ was discretized at steps of size 10^{-3}, and the boundary functions were evaluated on this mesh. The resulting coordinate pairs were passed to `polyshape`, along with the other points $(N, 0)$ and $(N, 1)$ on the right side of the domain.

The sinusoidal boundary functions were chosen to be $\phi_L(y) = \eta\cos(6\pi y)$ and $\phi_L(y) = \eta\sin(6\pi y)$, with the former being even and the latter odd about $y = \frac{1}{2}$. The hat functions were specified using `triangularPulse`, and the bump functions were specified as crests of a sine wave. Both of these boundary types had finitely many (usually two) hats/bumps, placed at varying y. The hats/humps had radius of 0.05, and positive amplitude. See Figure 2 for concrete examples.

Once the perturbed rectangular domain was specified, the Dirichlet problem for the Helmholtz equation was solved numerically. MATLAB offers a friendly user-interface for solving boundary value problems in its `PDE Toolbox`, but also offers a command-line interface for using it. Using this command-line interface, we first generate a finite-element mesh for the domain using `generateMesh` and solve the Helmholtz problem using `solvepdeeig`. The mesh resolution can be tuned via an argument to `generateMesh`, which is useful for ensuring a good rendering of the nodal set for larger domains.

For more details on the implementation, visit https://github.com/marichig/nodal-set-openings, which includes the code used for the following analyses as well as references to the relevant MATLAB documentation.

4.2. Effect of Symmetric Perturbation on Nodal Set Gap.

From our ansatz (1.5) and Prop. 1.2, we observed that choices of ϕ_L that are symmetric about $y = \frac{1}{2}$ would force $v_1(0)$, and consequently $v_1(x)$, to be small. In this case, any perturbation to the nodal set would be due to the exponentially small error term in (1.5).

Indeed, from the plots in Figure 3 (see further below) we see that the nodal set gap is smaller in the case of symmetric ϕ_L. That said, though the symmetric cases seem to show a crossing, it is unclear whether a crossing is truly present or if it is too small to detect at current numeric resolution.

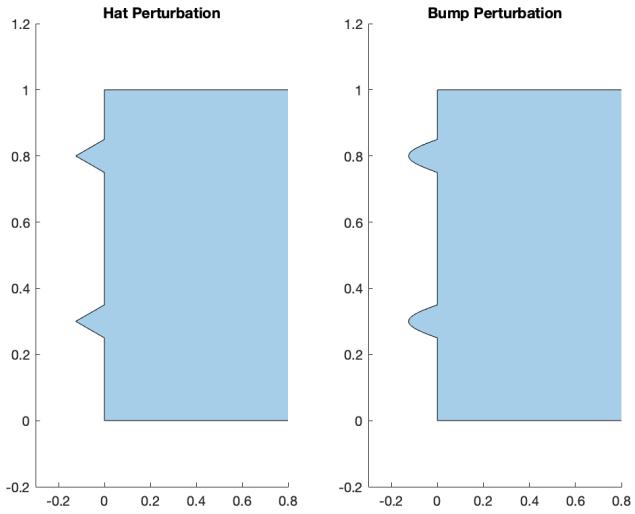

FIGURE 2. Example of a hat and bump perturbation. Each has two hat/bumps placed identically: one at $y = 0.3$ and the other at $y = 0.8$, both with radius 0.05 and amplitude 0.25.

4.3. **Change in Orientation about Resonant N.** According to Theorem 1.3, we see that the sign of $v(\frac{N}{2}, \frac{1}{2})$ determines the orientation of the nodal set. Further we recall from (1.9) and subsequent discussion that the sign of $v(\frac{N}{2}, \frac{1}{2})$ changed about $N \approx \frac{1}{\sqrt{3}} + \frac{2k}{\sqrt{3}}$.

To investigate this, we set $\phi_L(y) = \frac{1}{32}\sin(6\pi y)$, and consider aspect ratios close to (but not exactly) $N = 4.04$, which correspond to choice of $k = 3$. Since $\mu_1 > \sqrt{3}$, such an N will be an overestimate for the resonant value; we therefore investigate nearby N smaller than 4.04 to study the resonance effect. Indeed, exploration shows that the resonant value is close to $N \approx 3.85$ (see Figure 4).

The above shows that the nodal set switches orientation as the aspect ratio passes through a resonant value, where the axis along the opening changes from $[1, -1]^T$ to $[1, 1]$, and also shows a substantial deformation close to the resonant value. From running the numerical experiments, it was observed that in some simulations the index of the mode of study increased by 1 after passing by a resonant value, and that the eigenvalues of the $2-2$ mode and the displacing mode were close. Therefore, we speculate that this behavior may be due to a degenerate eigenvalue in the spectrum around such N where the $2-2$ mode gets displaced, but further work is needed to fully understand the behavior of the eigenfunction about such resonant aspect ratios.

4.4. **Nodal Set Gap Independence of N.** Lastly, as noted from Theorem 1.1, the separation along the x-axis is $O(\sqrt{\eta})$ and is independent of N. To verify this, we fix $\phi_L(y) = \frac{1}{2}\sin(6\pi y)$, and plot the desired mode on for various aspect ratios to see if the nodal gap remains comparable. Since the nodal set opening depends on N's relative position to a resonant value (as clear from Figure 4), we control for the resonance effect by choosing N such that $\left|\cos\left(\mu_1 \frac{N}{2}\right)\right| \approx 1$. (Accurately choosing such N is possible using MATLAB's calculated values for μ for each domain.) The mesh granularity is tuned for each domain to ensure that the maximum mesh element sizes are comparable across all tested aspect ratios. Moreover, using MATLAB's plotting tools, we manually identify the vertex of each nodal branch, which lets us roughly calculate the separation distance along the x-axis, d (see Figure 5, end of document, and Table 1).

The distances shown in Table 1 are comparable in order of magnitude across the various length-scales, and do not demonstrate a decreasing pattern for increasing N. This said, the experiments above may not be meaningful depending on whether the tested N were less than N_0, which may be quite large

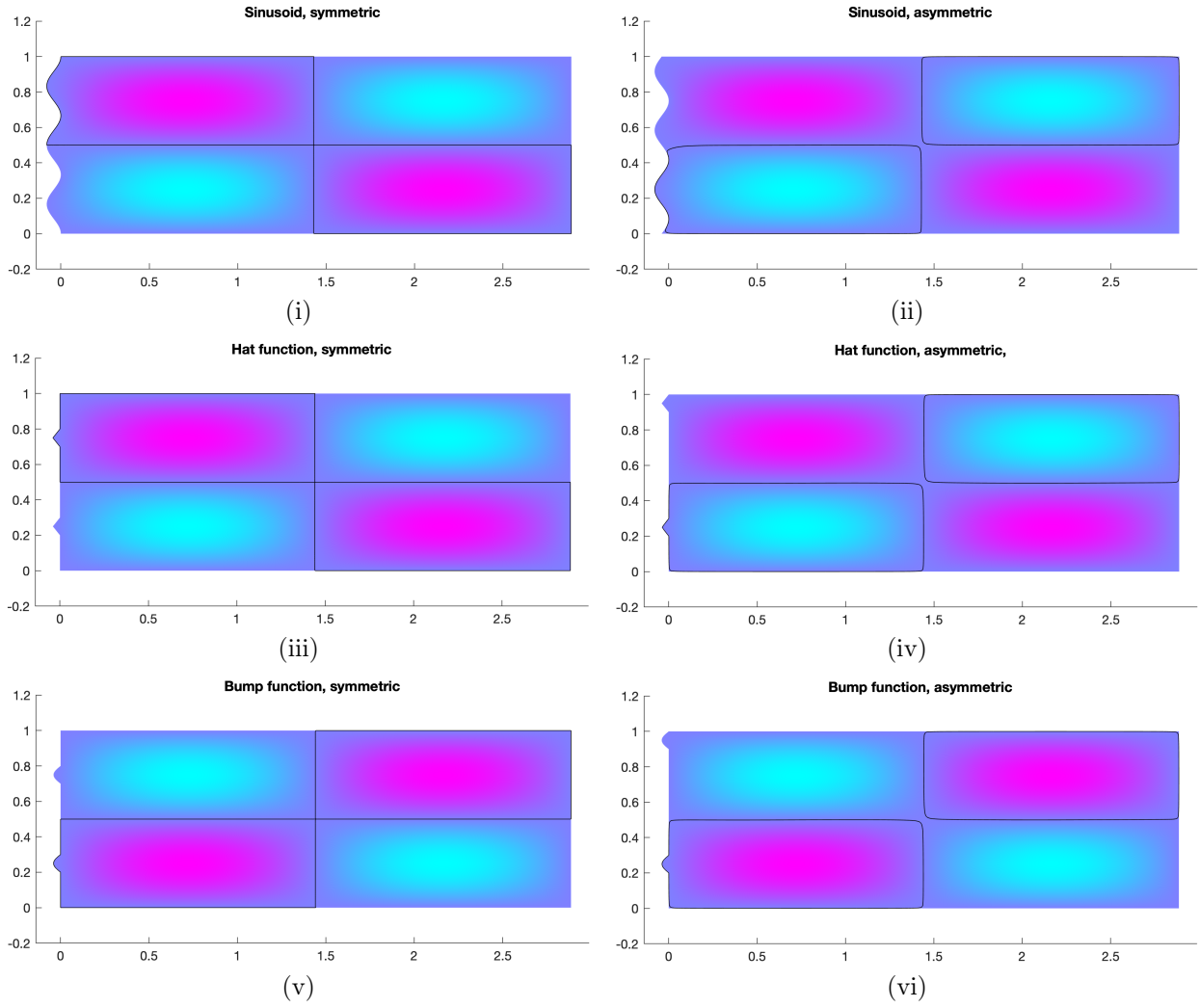

FIGURE 3. Symmetric and asymmetric boundary perturbation, $N = 5/\sqrt{3}$. In (i), (ii), the symmetric boundary is $\phi_L(y) = 0.04\cos(6\pi y)$ and the asymmetric, $\phi_L(y) = 0.04\sin(6\pi y)$. In (iii)-(vi), hats and bumps of radius 0.05 and amplitude 0.04, and are placed at $y = 0.25, 0.75$ in the symmetric boundary, and $y = 0.25, 0.95$ in the asymmetric.

depending on how efficient the bounds from Sections 2 and 3 were. While the above experiments for moderate N do not show dependence of d on the aspect ratio and lend support to the $O(\sqrt{\eta})$ estimate, more work is needed to numerically validate the nodal gap opening's asymptotic independence of N.

N	d	Max. Mesh Size ($\times 10^{-3}$)	μ	$\left\lvert\cos\left(\mu_1 \frac{N}{2}\right)\right\rvert$
5.7155	0.042	1.2431	40.6506	1.0000
11.56	0.045	1.206	39.7605	0.9998
23.0896	0.03	1.1795	39.5318	0.9999
46.2648	0.05	1.4029	39.476	1.0000

TABLE 1. Rough estimates for separation distance d along the $x-$axis from the plots in Figure 5, with mesh sizes, eigenvalues μ, and the size of resonance effect. Recall $\mu_1^2 = \mu - \pi^2$.

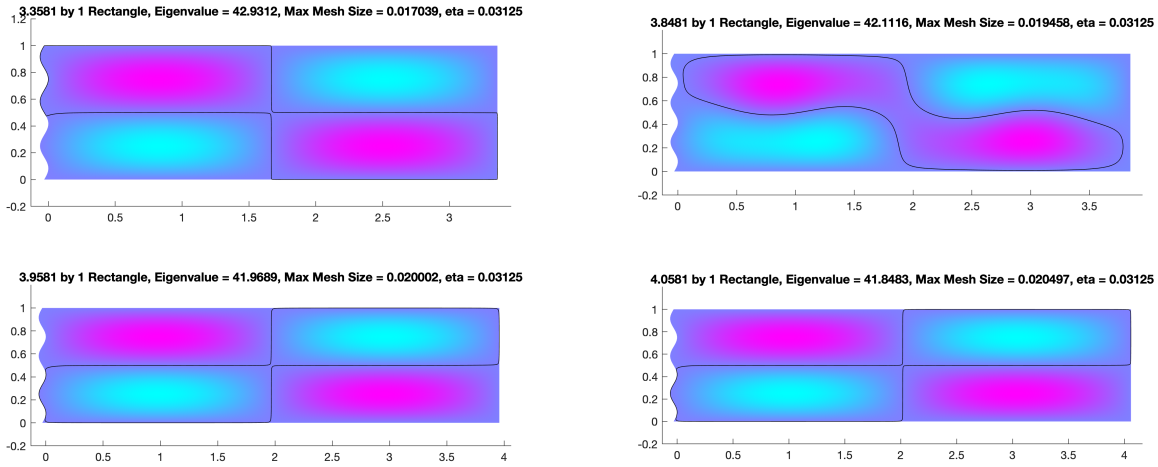

FIGURE 4. Plots around the resonant aspect ratio $N \approx 3.85$, with detail shown around the nodal opening.

REFERENCES

[1] Thomas Beck, Yaiza Canzani and Jeremy Marzuola. Nodal line estimates for the second Dirichlet eigenfunction. *Journal of Spectral Theory*, 2020.

[2] Pierre Bérard and Bernard Helffer, Dirichlet eigenfunctions of the square membrane: Courant's property, and A. Stern's and Å. Pleijel's analyses. *Springer Proceedings in Mathematics and Statistics*, 2015.

[3] Richard Courant and David Hilbert. Methods of Mathematical Physics: Vol. 1. *New York: Wiley*, 2nd Edition, 1989 (1st Edition, 1952). Statement of theorem is in Section VI.6, p. 452.

[4] Germán Lozada-Cruz. A simple application of the implicit function theorem. *Boletín de la Asociación Matemática Venezolana*, 2012.

[5] Daniel Grieser and David Jerison. Asymptotics of the first nodal line of a convex domain. *Inventiones mathematicae*, 1996.

[6] Daniel Grieser and David Jerison. The size of the first eigenfunction of a convex planar domain. *Journal of the American Mathematical Society*, 1998.

[7] Daniel Grieser and David Jerison. Asymptotics of eigenfunctions on plane domains. *Pacific Journal of Mathematics*, 2009.

[8] Luc Hillairet and Jeremy Marzuola. Nonconentration for partially rectangular billiards. *Analysis & PDE*, 2012.

[9] Åke Pleijel. Remarks on Courant's nodal line theorem. *Commun. Pure Appl. Math.*, 1956.

Email address: marichi@live.unc.edu

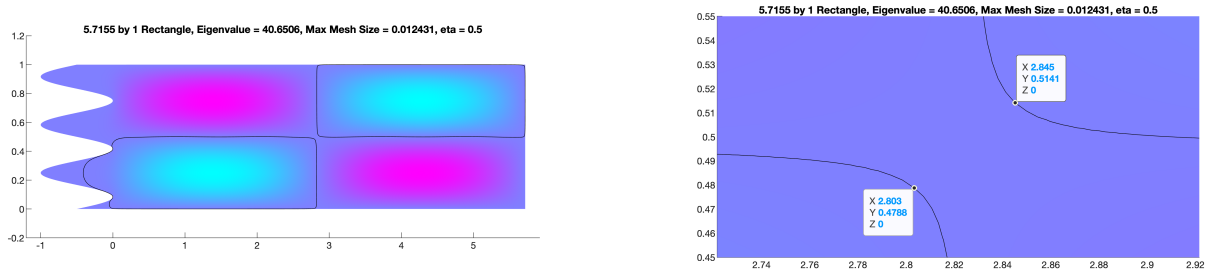

(i)

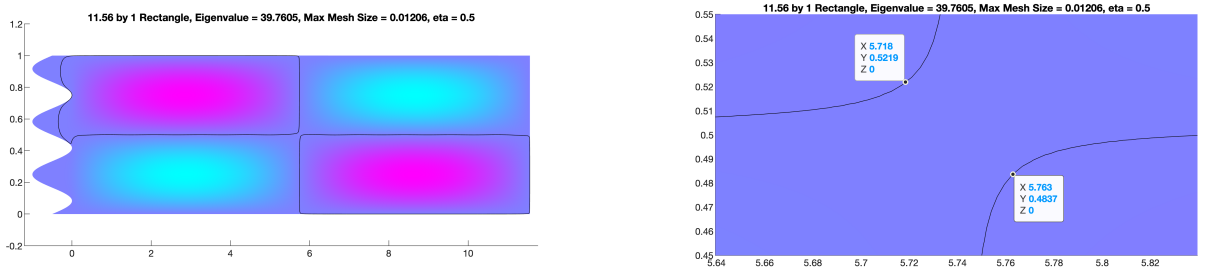

(ii)

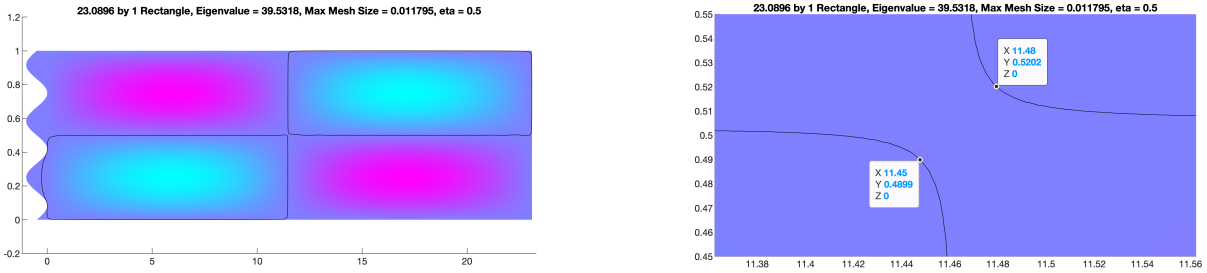

(iii)

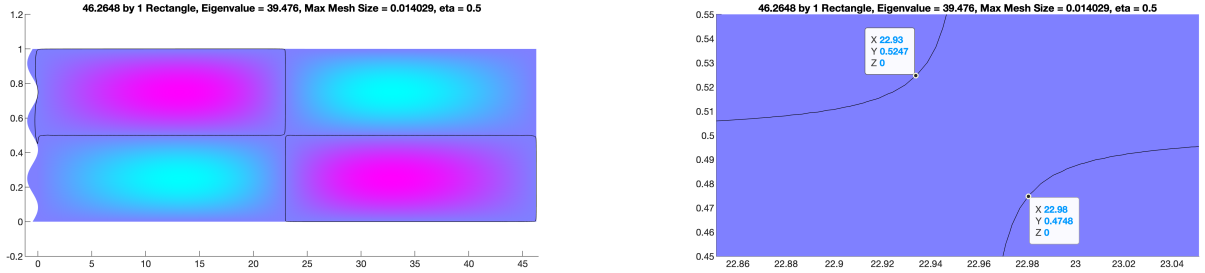

(iv)

FIGURE 5. Plots for varying aspect ratios with fixed boundary perturbation, as well as detail of the nodal opening. Vertex labels on the nodal branches are chosen manually by inspection.